

High Fidelity Reduced Order Models for Wildland Fires

Alan M. Lattimer*

Virginia Tech, Blacksburg, VA, USA, alattime@vt.edu

Brian Y. Lattimer

JENSEN HUGHES, Blacksburg, VA, USA, blattimer@jensenhughes.com

Serkan Gugercin

Virginia Tech, Blacksburg, VA, USA, gugercin@vt.edu

Jeffrey T. Borggaard

Virginia Tech, Blacksburg, VA, USA, jborggaard@vt.edu

Kray D. Luxbacher

Virginia Tech, Blacksburg, VA, USA, kraylux@vt.edu

Introduction

The modeling and simulation of fires is a complex, multi-scale problem. The need to create accurate models extends from prevention to prediction to damage control management. Since these problems are so complex, even models of moderately-sized fires in relatively small domains require significant computational resources and time to solve. Further, the actual physics are often difficult to model exactly, e.g. the exact fuel loading and distribution in a burning room or wildland fire. To this end, much of the focus in the fire community has been on simplifying the physics of the problem to obtain reasonable models. Current techniques for reducing fire models, such as proper orthogonal decomposition (POD) (see Kunisch and Volkwein [2002], Hinze and Volkwein [2005], Sharma et al. [2013], Volkwein [2013]), often have limited effectiveness due in large part to the inherent nonlinearities that exist in fire models. Regardless of the size of the reduced-order model (ROM), the nonlinearities must still be evaluated at the full-order of the model. This issue, referred to as the *lifting bottleneck*, must be addressed in order to fully realize the computational gains for a given reduced-order model. In this paper, we examine reduced-order modeling for two different fire models. For the wildland fire-spread model given by Mandel et al. [2008], we employ DEIM (see Chaturantabut and Sorensen [2010]) to address the computational bottleneck associated with the nonlinearity in the model. We then examine fire-plume models in relation to the underlying structure of the fire. Additionally, we evaluate the quality of the ROM with regards to capturing the essential features of the fire.

Wildland Fire-Spread Model

Large-scale models for real-time simulations, as required for predicting wildland fires, are avoided due to limited computational resources. On the other hand, lower spatial resolution limits the physics that can be captured by the models. Reduced-order modeling is an approach that retains the physics of the problem while simultaneously reducing the computational costs. The accuracy and improved computational efficiency are demonstrated by building a ROM for a wildland fire spread model.

*ICAM, 765 West Campus Dr., Blacksburg, VA, USA, alattime@vt.edu

Basic Description

We explored a reduced-order model (ROM) for the phenomenological model suggested in Mandel et al. [2008] to predict flame front propagation in wildland fires given by

$$\frac{\partial T}{\partial t} = \kappa \frac{\partial^2 T}{\partial x^2} - v \frac{\partial T}{\partial x} + \alpha \left(S e^{-\tilde{\beta}/(T-T_0)} - \gamma(T-T_0) \right), \quad (1)$$

$$\frac{\partial S}{\partial t} = -\gamma_S S e^{-\tilde{\beta}/(T-T_0)}, \quad (2)$$

where T is the temperature, and S is the mass fraction of fuel in a propagating fire. Using constant parameters and wind velocity, the nonlinearity of this model occurs via a reaction term.

Proper orthogonal decomposition (POD) is the most commonly used technique to produce ROMs for complex nonlinear dynamics Hinze and Volkwein [2005]. POD has been used to reduce wildland fire-spread models (e.g. Mandel et al. [2008]) in Sharma et al. [2013], Guelpa et al. [2014] to achieve modest gains in computational performance. Though ROMs using POD are effective, they can be significantly improved for nonlinear systems by addressing the so-called *lifting bottleneck* using the Discrete Empirical Interpolation Method (DEIM) described below. This lifting bottleneck occurs when computing the reduced nonlinear term, since standard POD first lifts the reduced variables up to the full-order dimension, evaluates the nonlinear term, then projects the result back down to reduced dimension. Therefore, the computational gains compared to the original model are limited since the nonlinear terms are computed at the full-order dimension.

Discrete Empirical Interpolation Method (DEIM)

Suppose we have a nonlinear system given by $\dot{\mathbf{x}}(t) = \mathbf{A}\mathbf{x}(t) + \mathbf{f}(\mathbf{x}(t))$ where $\mathbf{A} \in \mathbb{R}^{n \times n}$, $\mathbf{x} : \mathbb{R} \rightarrow \mathbb{R}^n$, and $\mathbf{f} : \mathbb{R}^n \rightarrow \mathbb{R}^n$. Suppose that $\mathbf{V} \in \mathbb{R}^{n \times r}$ is the projection matrix that we determine using POD. Then using a Galerkin projection we see that the ROM would be

$$\dot{\mathbf{x}}_r(t) = \underbrace{\mathbf{V}^T \mathbf{A} \mathbf{V}}_{\mathbf{A}_r: r \times r} \mathbf{x}_r(t) + \underbrace{\mathbf{V}^T}_{r \times n} \underbrace{\mathbf{f}(\mathbf{V} \mathbf{x}_r(t))}_{n \times 1}, \quad (3)$$

where $\mathbf{x}_r : \mathbb{R} \rightarrow \mathbb{R}^r$. For the nonlinear term, $\mathbf{x}_r(t)$ must be lifted back to the original size of the state space, i.e. $\mathbf{V} \mathbf{x}_r(t) \in \mathbb{R}^n$, before evaluating \mathbf{f} . This implies that the computational complexity of calculating the nonlinear term is order n .

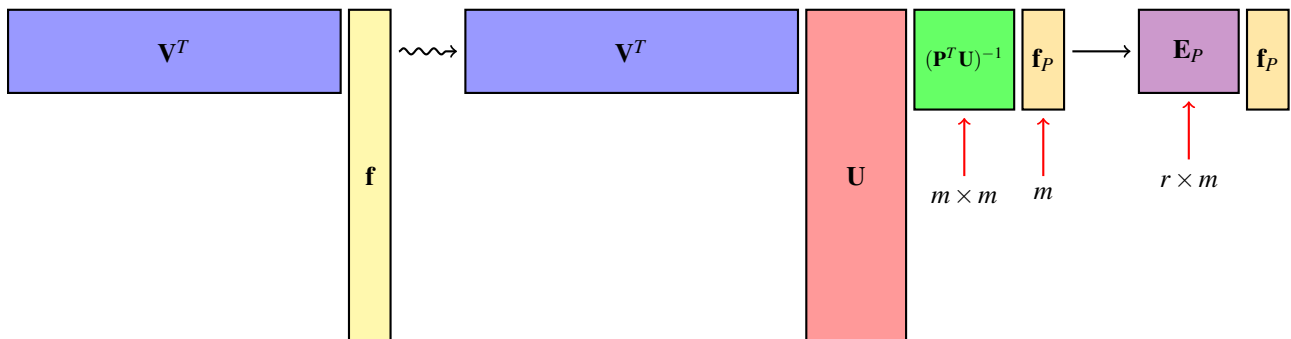


Figure 1: Visual depiction of the DEIM approximation $\mathbf{V}^T \mathbf{f}(t) \approx \mathbf{E}_P \mathbf{f}_P(t)$.

We can reduce this complexity by employing DEIM Chaturantabut and Sorensen [2010], a discrete variant of the Empirical Interpolation Method introduced in Barrault et al. [2004]. Given the nonlinear dynamics in (3) from the nonlinearity $\mathbf{f} : \mathbb{R}^n \rightarrow \mathbb{R}^n$, during a simulation, in addition to the snapshots of the state-vector \mathbf{x} , we collect snapshots of the nonlinearity \mathbf{f} . Then, we compute the DEIM-projection matrix \mathbf{U} as the leading left-singular vectors of the nonlinear snapshots, i.e., we compute a POD basis for the nonlinearity. Let $\mathbf{U} \in \mathbb{R}^{n \times m}$, where $m \ll n$. Then, the DEIM approximation of \mathbf{f} is given by

$$\widehat{\mathbf{f}}(t) = \mathbf{U}(\mathbf{P}^T \mathbf{U})^{-1} \mathbf{P}^T \mathbf{f}(t), \quad (4)$$

where \mathbf{P} is the $n \times m$ DEIM-selection operator, obtained by selecting certain columns of the $n \times n$ identity matrix \mathbf{I} . The reduced nonlinear term, then, becomes

$$\mathbf{f}_r(\mathbf{x}_r(t)) \approx \mathbf{V}^T \mathbf{U}(\mathbf{P}^T \mathbf{U})^{-1} \mathbf{P}^T \mathbf{f}(\mathbf{V} \mathbf{x}_r(t)). \quad (5)$$

We emphasize that, in contrast to the analytical formula given by (5), for a numerical implementation, one computes $\mathbf{f}_r(\mathbf{x}_r(t))$ without lifting $\mathbf{x}_r(t)$. Instead, one evaluates $\mathbf{f}_r(\mathbf{x}_r(t))$ at selected rows of $\mathbf{V} \mathbf{x}_r(t)$. The selection operator \mathbf{P} enforces interpolation at the selected indices of \mathbf{f} , called the DEIM indices, and those indices are computed via a greedy search process. When we have a component-wise nonlinearity, as we do here, we can move \mathbf{P} into the nonlinear function. We can then define $\mathbf{E}_P := \mathbf{V}^T \mathbf{U}(\mathbf{P}^T \mathbf{U})^{-1}$ and $\mathbf{f}_P(t) := \mathbf{f}((\mathbf{P}^T \mathbf{V}) \mathbf{x}_r(t))$, where $\mathbf{E}_P \in \mathbb{R}^{r \times m}$ and $(\mathbf{P}^T \mathbf{V}) \in \mathbb{R}^{m \times r}$ only have to be computed once. For details, we refer the reader to the original source Chaturantabut and Sorensen [2010]. In our implementation, we employ a new variant of DEIM recently developed by Drmac and Gugercin [2015] where the greedy search is performed via a pivoted QR decomposition.

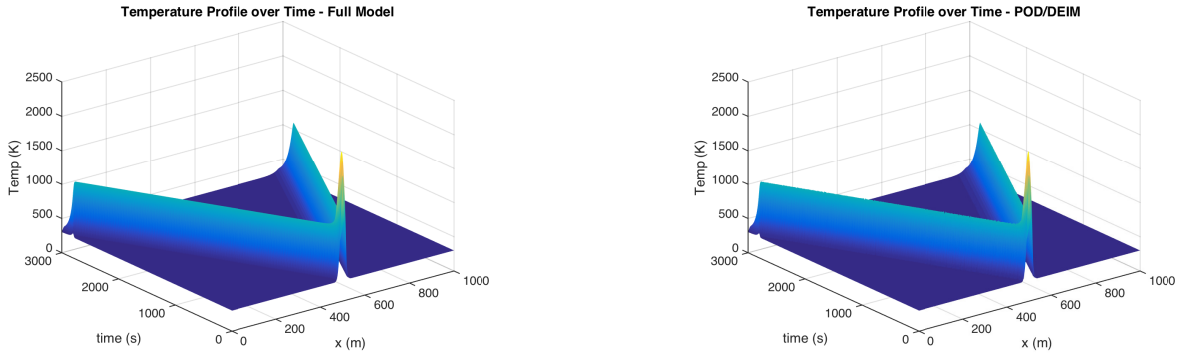


Figure 2: FOM versus the POD/DEIM ROM where $r_T = 250$, $r_S = 150$, and $r_{DEIM} = 250$.

Methods and Numerical Results

For the wildland fire-spread model (1)-(2), we can discretize the system using finite differences to create the following discretized model

$$\begin{bmatrix} \dot{\mathbf{T}}(t) \\ \dot{\mathbf{S}}(t) \end{bmatrix} = \begin{bmatrix} \mathbf{A}_T & \mathbf{0} \\ \mathbf{0} & \mathbf{0} \end{bmatrix} \begin{bmatrix} \mathbf{T}(t) \\ \mathbf{S}(t) \end{bmatrix} + \begin{bmatrix} \alpha \mathbf{f}[\mathbf{T}(t), \mathbf{S}(t)] \\ -\gamma_S \mathbf{f}[\mathbf{T}(t), \mathbf{S}(t)] \end{bmatrix}, \quad (6)$$

where $\mathbf{f}[\mathbf{T}(t), \mathbf{S}(t)] = \mathbf{S}(t) e^{-\beta/(\mathbf{T}(t)-T_0)}$ is the nonlinear function that is approximated using DEIM. Additionally, separate POD bases were built for the temperature and fuel mass fractions. This

also saved computational costs since the fuel mass fraction did not require as many basis vectors to accurately represent the results. For our testing we used the parameter values specified in Mandel et al. [2008], and the system was discretized from 0 to 1000 m in 0.2 m increments and solved over 3000 s. The initial condition has a fire at the 500 m location. The fire then propagates across the domain towards both boundaries based on equations (1-2) as seen in Figure 2.

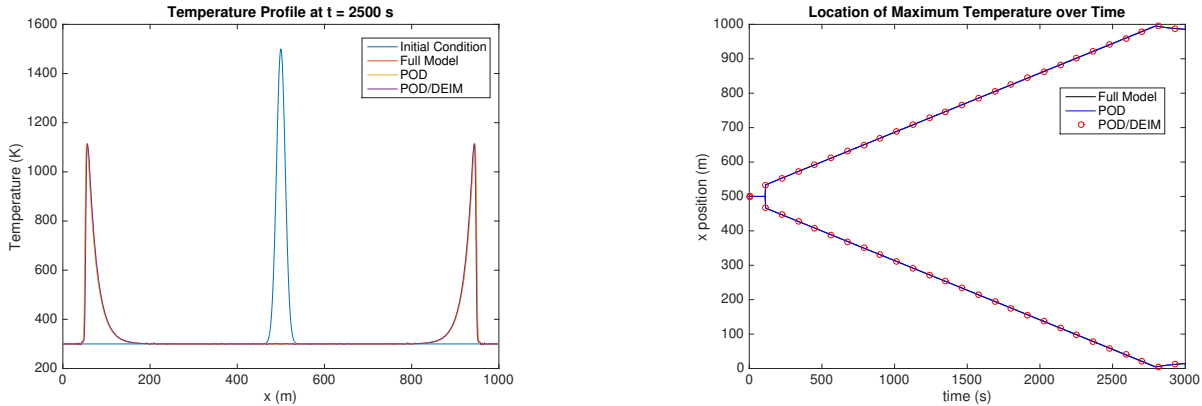


Figure 3: Fire spread for FOM, POD, and POD/DEIM.

Using the data snapshots created, r_T and r_S number of POD bases for T and S , respectively, were created. Further, POD was enhanced by projecting the nonlinearity using 250 DEIM vectors. Figures 2 and 3 show that the POD/DEIM ROM provides an excellent approximation of the full-order model (FOM) matching both the flame front location and temperature profile quite well.

Table 1: Results for the ROM. Solution time for the FOM was 99.1 s

# POD Vectors	POD			POD/DEIM		
	$r_T/r_S/r_{DEIM}$	Time (s)	Speed up	Rel Error	Time (s)	Speed up
70/35/250	1.33	74.6	1.7471e-02	0.13	760.1	1.7594e-02
200/150/250	15.4	6.38	4.3329e-03	0.72	137.6	5.2877e-04
200/200/250	18.5	5.31	1.8478e-02	0.84	118.2	1.3873e-02

As shown in Table 1, the solution times increase when more POD/DEIM vectors are used, but even the largest ROM using POD only was five times faster than the FOM. Further the relative error between the full-order and reduced-order model solutions was less 2% in all cases with a minimum of 0.43% when using 200 POD vectors for T and 150 POD vectors for S . When using POD with DEIM, the solution times were significantly better than POD alone while maintaining essentially the same error. The results demonstrate that using POD with DEIM can reduce the computational time by 2-3 orders of magnitude while retaining the physics and prediction accuracy.

Fire Plumes

Fire-plume simulations involve fine scale discretizations of coupled nonlinear PDEs. The complexity of the simulations are such that one cannot expect reduced-order models to accurately capture every feature of the simulations. In fact, a fundamental premise of reduced-order modeling in these cases is an underlying low-dimensional manifold for the full-order simulation.

However, many of the applications of fire modeling do not require knowledge of the states at every point in time and space, but rather they need to capture certain characteristics of the fire that would be useful for either making safety design decisions or to evaluate real-time fire suppression strategies. When considering how well a ROM of a fire matches the full-order fire model, we consider the following: 1) Dynamics, 2) Magnitude, and 3) Oscillation frequency and amplitude. We see that these criteria do not seek to strictly minimize an error between the FOM and ROM at some particular time step, but they do measure the efficacy of the ROM in representing the fire.

Description and Methods

Using the Fire Dynamics Simulator (FDS) software we generated a 2D full-order model of a 40 kW methane plume fire. Data was captured for 500 time steps evenly spaced over 20 seconds. To produce a ROM for this data, we used the PDE in (7)-(9) for our model.

$$\frac{\partial \mathbf{u}}{\partial t} = -\mathbf{u} \cdot \nabla \mathbf{u} - \nabla p + \nu \nabla^2 \mathbf{u} - \beta \mathbf{g}(T - T_\infty), \quad (7)$$

$$0 = \nabla \cdot \mathbf{u}, \quad (8)$$

$$\frac{\partial T}{\partial t} = -\mathbf{u} \cdot \nabla T + \alpha \nabla^2 T. \quad (9)$$

In particular, we wanted to investigate how close we could get to the actual fire model without

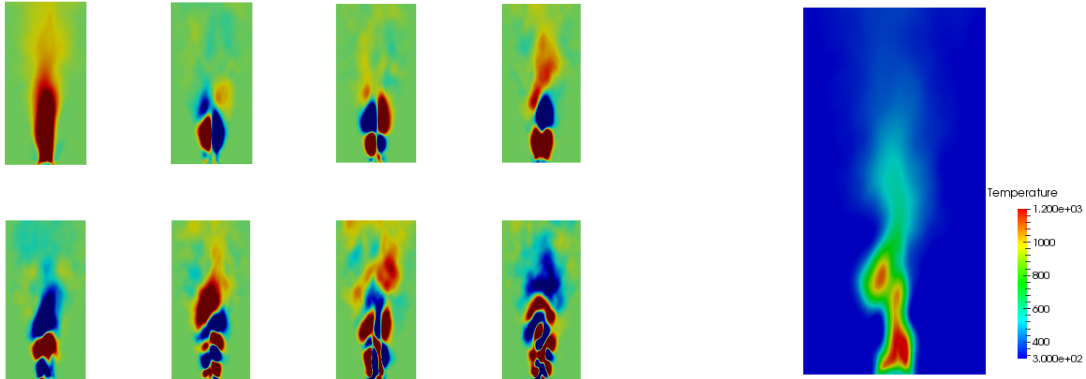


Figure 4: The left image shows the temperature POD modes for the small plume fire. Here we show POD modes 1, 2, 3, 4, 5, 10, 15, and 20 from left to right, top to bottom. On the right we show a typical reconstructed image created from the POD modes.

incorporating the combustion. From the snapshots, we created r POD basis modes for the u velocity, v velocity, and temperature T and used them to project the full-order PDE. Looking at the POD modes in Figure 4, we see that even though a fire seems to have random behavior, there are some underlying structures that exist. Further, the initial POD modes capture the overall shape and distribution of the fire, whereas the higher modes capture the finer details. The ROM seems to do a good job of capturing the dynamics of the system. While not exact, we do see the types of the oscillations of the mean and maximum temperatures and velocities indicative of a fire. The model was not quite as good at approximating the mean or maximum of the temperature or velocity. This is most likely due to the contribution of combustion in the FOM. Finally, the frequency of the temperature and velocity oscillations matches the FOM very well. However, the amplitudes of the oscillations were not as large as the FOM. Overall, the ROM does a good job of cap-

turing the fire dynamics, but to truly match the magnitude of the fire, the combustion aspect will need to be incorporated.

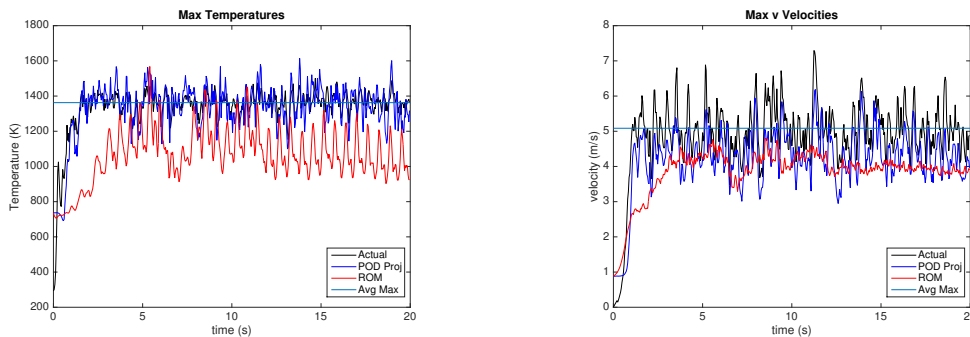


Figure 5: Maximum temperature and vertical velocity comparison between ROM and FOM with $r = 20$.

Acknowledgements

This research was partially developed under Grant No. 200-2014-59669, awarded by NIOSH. The findings and conclusions in this report are those of the authors and do not reflect the official policies of the Department of Health and Human Services; nor does mention of trade names, commercial practices, or organizations imply endorsement by the U.S. Government.

References

- Maxime Barrault, Yvon Maday, Ngoc Cuong Nguyen, and Anthony T. Patera. An ‘empirical interpolation’ method: application to efficient reduced-basis discretization of partial differential equations. *Comptes Rendus Mathematique*, 339(9):667–672, 2004.
- Saifon Chaturantabut and Danny C. Sorensen. Nonlinear model reduction via discrete empirical interpolation. *SIAM Journal on Scientific Computing*, 32(5):2737–2764, 2010.
- Zlatko Drmac and Serkan Gugercin. A New Selection Operator for the Discrete Empirical Interpolation Method—improved a priori error bound and extensions. *arXiv preprint arXiv:1505.00370*, 2015.
- Elisa Guelpa, Adriano Sciacovelli, Vittorio Verda, and Davide Ascoli. Model reduction approach for wildfire multi-scenario analysis. *Parte: <http://hdl.handle.net/10316.2/34013>*, 2014.
- Michael Hinze and Stefan Volkwein. Proper orthogonal decomposition surrogate models for nonlinear dynamical systems: Error estimates and suboptimal control. In *Dimension Reduction of Large-Scale Systems*, pages 261–306. Springer, 2005.
- K. Kunisch and Stefan Volkwein. Galerkin proper orthogonal decomposition methods for a general equation in fluid dynamics. *SIAM Journal on Numerical analysis*, 40(2):492–515, 2002.
- Jan Mandel, Lynn S. Bennethum, Jonathan D. Beezley, Janice L. Coen, Craig C. Douglas, Minjeong Kim, and Anthony Vodacek. A wildland fire model with data assimilation. *Mathematics and Computers in Simulation*, 79(3):584–606, 2008.
- Balaji R. Sharma, Manish Kumar, and Kelly Cohen. Spatio-Temporal Estimation of Wildfire Growth. In *ASME 2013 Dynamic Systems and Control Conference*, pages V002T25A005–V002T25A005. American Society of Mechanical Engineers, 2013.
- Stefan Volkwein. Proper orthogonal decomposition: Theory and reduced-order modelling. *Lecture Notes, University of Konstanz*, 2013.